New Route of Preparation and Properties of $NaNiO_2$

Mikhail Sofin and Martin Jansen

Max-Planck-Institut für Festkörperforschung,
Heisenbergstraße 1, D-70569 Stuttgart, Germany

Reprint requests to M. Jansen.
E-mail: m.jansen@fkf.mpg.de

Z. Naturforsch. **60b,** 701 – 704 (2005);
received January 26, 2005

$NaNiO_2$ was prepared through oxidation of a Na_2NiO_2/NiO mixture (1:1) in dried oxygen at 500 °C. Single crystals have been grown by annealing of $NaNiO_2$ powder at 600 °C for 83 d in a flow of dried oxygen. According to the X-ray analysis of the crystal structure ($C2/m$, $Z = 2$, $a = 5.3177(2)$, $b = 2.8458(1)$, $c = 5.5819(3)$ Å, $\beta = 110.409(2)^\circ$, R_1(all) = 3.4%, 185 independent reflections), the Jahn-Teller distorted NiO_6 octahedra, sharing edges, build up layers lying parallel to the *ab* plane. A phase transition (associated with an energy of 2.9 kJ/mole) to a high temperature rhombohedral form ($R\bar{3}m$, $Z = 3$, $a = 2.958(1)$, $c = 15.748(2)$ Å, at 300 °C) was observed by Guinier and DSC measurements at 195 °C. The magnetic susceptibility of the monoclinic phase can be described by the Curie-Weiss law between 100 and 330 K: $\mu = 2.01\mu_B$ (g = 2.32), $\Theta = 37$ K, indicating the dominance of ferromagnetic interactions of $S = 1/2$ spins within the NiO_2 layers. Antiferromagnetic interlayer interactions produce an overall antiferromagnetically ordered structure below 18 K.

Key words: Sodium Nickel Oxide, Crystal Structure, Magnetic Properties, Azide/Nitrate Route, DSC

Introduction

Compounds with layered structures are presently attracting high attention. Superconducting cuprates [1], manganates with colossal magnetoresistance [2] as well as electrode materials in batteries [3] posses this structural peculiarity. The most widely applied compounds in the latter materials' class are lithium and sodium manganates and cobaltates having the general formula $A_{1-x}MO_2$ (A = Li, Na, M = Mn, Co). Layers in these compounds are triangular and built up from edge-sharing MO_6 octahedra. Besides the research activities on battery materials (mostly as $Li_{1-x}CoO_2$ [3]) the triangular layered compounds are of particular interest because of magnetic frustration [4], and superconductivity phenomena recently found for hydrated $Na_{1-x}CoO_2$ [5]. Although $A_{1-x}NiO_2$ niccolates also have triangular layers, only a few investigations have been carried out on this family of compounds. For $NaNiO_2$ even a conventional X-ray single crystal analysis is still lacking. The structure of $NaNiO_2$ was determined first in 1954 by film methods using a precession camera [6] and refined later by Rietveld methods applying X-ray and neutron radiation [7]. A phase transition to a high temperature rhombohedral form at about 220 °C was established by DTA and Debye-Scherrer photographs [6]. In a single work on magnetism of $NaNiO_2$ [8], it was found that the substance shows a Curie-Weiss behaviour with $\mu = 1.74\mu_B$ and $\Theta = 90$ K showing the low-spin configuration of Ni^{+3}, which is retained after the transition into the rhombohedral form. However, the accuracy of the magnetic parameters obtained is questionable, as was admitted by the authors. In this work we present a new way of synthesis and additional investigations on $NaNiO_2$, which shows interesting physical properties.

Experimental Section

$NaNiO_2$ was synthesised in two steps. First, a mixture of Na_2NiO_2 [9] and NiO (in molar ratio 1:1) was prepared via the azide/nitrate route [10]. Starting materials for the preparation were nickel(II) oxide (Aldrich, 99.99%), sodium azide (Sigma-Aldrich, 99.99%) and sodium nitrate (Merck, 99.99%). The precursors (NiO, NaN_3 and $NaNO_3$) were mixed in the ratio required according to eq. (1), milled in a ball mill, pressed into pellets under 10^5 N, dried under vacuum (10^{-3} mbar) at 150 °C for 12 h, and placed under argon in a tightly closed steel container provided with a silver inlay [11]. In a flow of dry argon the following temperature profile was applied: 25 → 260 °C (100 °C/h); 260 → 380 °C (5 °C/h); 380 → 450 °C (10 °C/h), and subsequent annealing for 50 h at 450 °C. (Caution: if heated too rapidly, the containers may blow up!) Before the second step, the obtained powder was homogenized again by grinding in a glove box and pressed into pellets. The pellets were annealed for 10 h in silver crucibles, in a flow of dried oxygen (eq. (2)). The as obtained black powder is sensitive to humid air at storage and should be handled in an inert atmosphere.

$$5NaN_3 + NaNO_3 + 6NiO = 3Na_2NiO_2 + 3NiO + 8N_2 \quad (1)$$

$$Na_2NiO_2 + NiO + 1/2O_2 = 2NaNiO_2 \quad (2)$$

Single crystals were grown by annealing of $NaNiO_2$ powder at 600 °C for 83 d in a flow of dried oxygen.

T [°C]	SG	a [Å]	b [Å]	c [Å]	β/γ [°]	V [Å^3]
20	$C2/m$	5.323(1)	2.845(1)	5.584(1)	110.493(3)	79.21(1)
185	$C2/m$	5.315(1)	2.848(1)	5.588(1)	110.357(6)	83.56(1)
205	$R\bar{3}m$	2.956(1)	$= a$	15.732(2)	120	119.05(2)
300	$R\bar{3}m$	2.958(1)	$= a$	15.748(2)	120	119.33(2)

Table 1. Cell parameters and volume for $NaNiO_2$ depending on temperature according to the Guinier measurements.

The X-ray investigation on a powder sample was performed on a STOE Stadi P diffractometer with Cu-$K_{\alpha 1}$ radiation ($\lambda = 1.54178$ Å) at room temperature using a position sensitive detector and a curved germanium monochromator. Temperature-dependent X-ray measurements on a powder sample were performed on a Guinier camera (FR 553, Enraf-Nonius). The sample was heated from room temperature up to 300 °C with a rate of 15 °C/h and afterwards cooled down to room temperature with the same rate. The single crystal diffraction data were collected on a three-cycle diffractometer (Bruker AXS), equipped with a SMART-CCD (APEX), at 293 K.

Magnetic measurements were performed on a SQUID-Magnetometer (MPMS 5.5, Quantum Design) between 5 and 330 K in magnetic fields up to 5 T. The diamagnetic correction was applied using tabulated values [12].

Thermal analyses were carried out using a DSC device (DSC 404, Netzsch) in a Pt crucible covered with a Pt lid. The sample (m = 80.5 mg) was heated under dry argon up to 400 °C at a rate of 10 K/min and then cooled down with the same rate. Elementary tin was used as a reference for the measurement of the heat of transition.

Results and Discussion

$NaNiO_2$ was prepared in two steps as a pure microcrystalline powder. The black product is sensitive to moist air, and must be kept in an inert atmosphere.

The X-ray powder diffraction pattern of the single phase product could be indexed monoclinicly with lattice constants $a = 5.3177(2)$, $b = 2.8458(1)$, $c = 5.5819(3)$ Å, $\beta = 110.409(2)^\circ$. The crystal structure of the sodium niccolate, which crystallises in the space group $C2/m$, was determined from a single crystal. The most remarkable structural feature is NiO_2 layers composed of edge-sharing NiO_6 octahedra and aligned in the *ab* plane (Fig. 1). The NiO_6 octahedra are elongated due to Jahn-Teller distortion. The distortion, expected for the low-spin d^7 configuration in octahedral surrounding, is remarkably strong – 13% (apical Ni-O bond lengths 2.16 Å, basal ones 1.91 Å). Sodium ions lying between NiO_2 slabs are also coordinated octahedrally by oxygen atoms, but the distortion is negligible, being mostly compensated by the mutual shift of the layers. In general, the structure established in this work [13] is in good agreement with the result of previous investigations [6, 7], but the single crystal data presented here are of higher

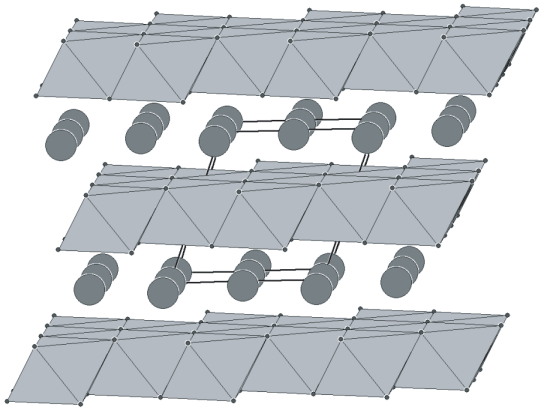

Fig. 1. Crystal structure of $NaNiO_2$ (room temperature form), emphasising the layers of edge sharing NiO_6 octahedra and of intercalated sodium atoms.

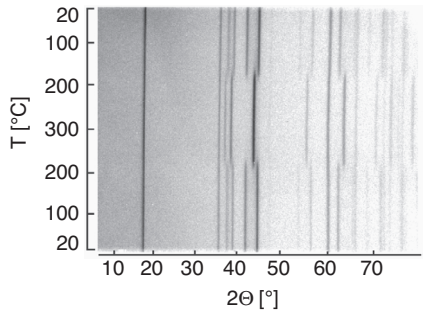

Fig. 2. Temperature-dependent diffraction pattern of $NaNiO_2$ (20 °C → 300 °C → 20 °C, heating/cooling rate: 15 °C/h).

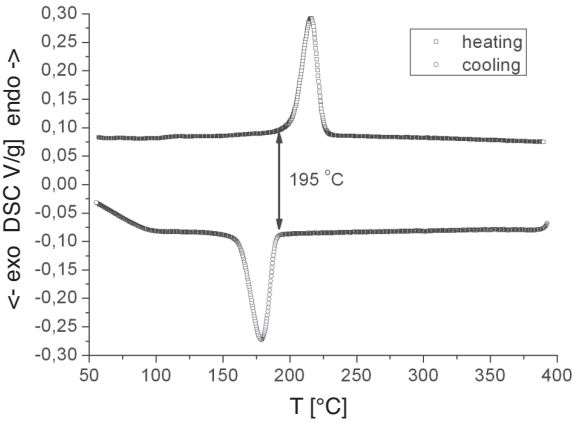

Fig. 3. DSC measurements for $NaNiO_2$ (circles: heating, squares: cooling).

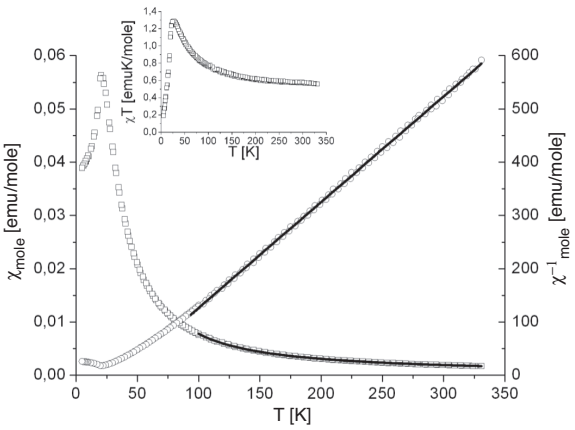

Fig. 4. Magnetic susceptibility of $NaNiO_2$ represented as χ *vs.* T (squares) and χ^{-1} *vs.* T (circles). The full line corresponds to the fit by the Curie-Weiss law. Inset: χT *vs.* T.

precision by at least one order of magnitude. This room temperature form of $NaNiO_2$ is isostructural to $NaMnO_2$ [14, 15].

In order to follow the phase transition, a temperature dependent diffraction pattern was recorded (Fig. 2). At about 195 °C the symmetry reduction due to the static Jahn-Teller effect is overcome by thermal motion, and the phase turns into a rhombohedral form [6] which is isostructural with α-$NaFeO_2$ [16] or $LiNiO_2$ [6] (rock salt variant). The cell parameters just before and after the transition, as well as at the highest temperature measured (300 °C), are given in Tab. 1. The DSC measurements have confirmed (Fig. 3) that this transition occurs at 195 °C, is endothermic on heating with a latent heat of 2.9 kJ/mole, and shows a hysteresis of 40 °C at the heating/cooling rate of 10 °C/min. Our findings are different from the published transition temperature (220 °C) [6], but the maximum on the DSC heating curve corresponds to this value, what is probably to be explained by a previously unattended transition hysteresis.

The magnetic susceptibility was measured on a powder sample in the range 5 – 300 K at magnetic fields from 0.001 to 5 T. The susceptibility data, which are essentially independent of the field strength, are shown in Fig. 4 for 0.1 T. The effective magnetic moment at 300 K ($\mu = 2.15\mu_{\mathrm{B}}$, $\mu_{\mathrm{spin\,only}} = 1.73\mu_{\mathrm{B}}$) and the growth of χT values with dropping temperature indicate the low-spin state of the Ni^{+3} ions (d^7) and the dominance of a ferromagnetic spin interaction in the system. The χT curve (inset in Fig. 4) reaches its maximum at 25 K and than sharply decreases to zero showing that the final ordered state is antiferromagnetic. The Néel temperature is 18 K (maximum in $\partial\chi/\partial T$). Taking into account the layered structure of $NaNiO_2$, one can assume that the dominant ferromagnetic interaction is due to the in-plane spin exchange, while the three-dimensional, antiferromagnetically ordered low-temperature state is a consequence of weaker antiferromagnetic interlayer interactions. In spite of the complex character of the magnetic interactions, the susceptibility could be described by the Curie-Weiss law in the range 100 – 330 K. Below 100 K the χ^{-1} curve diverges remarkably from the linear behaviour indicating a presence of strong antiferromagnetic interlayer interactions. A least-squares fit of the χ^{-1} data yields: $\mu = 2.01\mu_{\mathrm{B}}$, $\Theta = 37$ K and the full lines in Fig. 4. The parameter obtained are in good agreement with the above qualitative discussion. Compared to the data of a previous investigation ($\mu = 1.74\mu_{\mathrm{B}}$, $\Theta = 90$ K) [8], our magnetic moment is essentially higher and seems to be more plausible, since one normally finds a larger value (compared to the spin-only one) for a d^7 configuration due to the spin-orbit coupling effect. Furthermore, the too low value of the magnetic moment reported previously leads to a higher Weiss constant, probably indicating a fitting inaccuracy caused by the low precision of the Faraday method used in [8].

Acknowledgements

We would like to thank E. Brücher, J. Nuss, D. Orosel, N. Sofina for experimental assistance.

[1] L. J. Masur, J. Kellers, F. Li, S. Fleshler, E. R. Podtburg, IEEE T. Appl. Supercon. **12**, 1145 (2002).
[2] C. N. R. Rao, A. K. Cheetham, R. Mahesh, Chem. Mater. **8**, 2421 (1996).
[3] R. Kanno, Electrochemistry **71**, 713 (2003).
[4] H. Lueken, Magnetochemie, Teubner, Stuttgart (1999).
[5] K. Takada, H. Sakurai, E. Takayama-Muromachi, F. Izumi, R. A. Dilanian, T. Sasaki, Nature **422**, 53 (2003).
[6] L. D. Dyer, B. S. Borie, G. P. Smith, J. Am. Chem. Soc. **76**, 1499 (1954).
[7] S. Dick, M. Müller, F. Preissinger, T. Zeiske, Powder Diffraction **12**, 239 (1997).
[8] P. F. Bongers, U. Enz, Solid State Comm. **4**, 153 (1966).
[9] H. Zentgraf, R. Hoppe, Z. Anorg. Allg. Chem. **462**, 71 (1980).
[10] D. Trinschek, M. Jansen, Angew. Chem. **111**, 234 (1999); Angew. Chem. Int. Ed. **38**, 133 (1999).
[11] M. Sofin, E.-M. Peters, M. Jansen, Z. Anorg. Allg. Chem. **628**, 2697 (2002).
[12] Landolt-Börnstein, Zahlenwerte und Funktionen aus Naturwissenschaften und Technik; Neue Serie, Gr. II, Bd. 2, Springer, Berlin (1966).
[13] Crystal data (293 K): monoclinic, $C2/m$ (No. 12), $Z = 2$, $a = 5.3177(2)$, $b = 2.8458(1)$, $c = 5.5819(3)$ Å,

$\beta = 110.409(2)^\circ$, $M_w = 113.7$, $\varrho = 4.77$. Single crystal X-ray structure determination: Intensities were measured with graphite-monochromatized Mo-K_α radiation ($\lambda = 0.71069$ Å) on a Bruker AXS Diffraktometer with APEX Smart CCD; 185 independent reflections (434 total measured) were analyzed by direct methods. The refinement by full-matrix least-squares gave final values R_1(all) = 0.034, wR_2(all) = 0.091. Further details on the crystal structure investigation are available from the Fachinfomationszentrum Karlsruhe, D-76344 Eggenstein-Leopoldshafen (Germany) on quoting the depository number CSD-415072, the name of the authors, and citation of the papers.

[14] J. P. Parant, R. Olazcuaga, M. Devalette, C. Fouassier, P. Hagenmuller, J. Solid. State. Chem. **3**, 1 (1971).
[15] M. Jansen, R. Hoppe, Z. Anorg. Allg. Chem. **399**, 163 (1973).
[16] Y. Takeda, K. Nakahara, M. Nishijima, N. Imanishi, O. Yamamoto, M. Takano, Mater. Res. Bull. **29**, 659 (1994).